

Improved Control Design Methods for Proximate Time-Optimal Servomechanisms

Aurélio T. Salton, Zhiyong Chen, and Minyue Fu, *Fellow, IEEE*

Abstract—It is well known that minimum time-optimal control for servomechanisms can generate chattering in the presence of measurement noises, feedback delays, or model uncertainties; thus, it is not practical in applications. Maybe, the most popular alternative approach is the so-called proximate time-optimal servomechanism (PTOS). This approach starts with a near-time-optimal controller and, then, switches to a linear controller when the system output is close to a given target. However, the chattering problem is avoided at the expense of a slower time response. In this paper, two methods for eliminating the conservatism present in the PTOS are proposed. The first method applies a dynamically damped controller that allows the so-called acceleration discount factor to be pushed arbitrarily close to 1. The second method applies a continuous nonlinear control law that makes use of no switching. Experimental results show that the proposed designs practically eliminate the conservatism in the traditional PTOS.

Index Terms—Motion control, nonlinear feedback, time-optimal performance.

I. INTRODUCTION

TIME-OPTIMAL performance, or minimum time point-to-point motion, is the objective of countless automatic control systems. Hard disk drives (HDDs), pick and place manipulation tools, robot arm control, automatic assembly stations, and many other precision engineering problems are the applications that benefit from it.

Unfortunately, it is well known that time-optimal control (TOC) strategies [1] suffer from chattering [2] and are unable to deliver the solution in a practical sense. A different strategy is necessary in order to achieve fast seek time motion. The main objective of this paper is to develop a controller that is able to

achieve near-time-optimal performance for rigid-body systems in a practical feedback structure.

The interest in rigid-body systems comes from the wide range of plants that are described by this particular dynamic model. Electromagnetic motors, for example, are some of the most common actuators used in precision engineering and are commonly described by rigid-body equations of motion [3]. Many HDD systems are also modeled by this particular set of equations, both as a single-stage HDD [4] and as the primary stage of a dual-stage HDD [5]–[7]. In particular, it is the primary actuator of dual-stage actuators (DSA) that the main motivation of this paper comes from. The present study may be considered an extension of the work on preview control for DSA [8], and an adaption of the design proposed in this paper may be applied to that class of systems as well. However, independent of the specific plant in hand, every system is inherently driven by a limited control input. Due to this fact, optimal performance remains a challenge inasmuch as a form of nonlinear control must be investigated in order to take into account the effects of control input saturation.

To overcome the chattering problem in TOC caused by measurement noises, feedback delays, and model uncertainties, a modified technique was proposed by Workman under the name of proximate time-optimal servomechanism (PTOS) [9]–[11]. Certainly, the most important work toward time optimal performance of servo systems, the PTOS, overcomes the problems related to TOC by using the maximal acceleration of the actuator only when it is practical to do so. As the system output approaches the reference point, the controller switches to a linear control law, thus eliminating chattering and providing feedback in order to accommodate plant uncertainty and measurement noise. This controller became very popular in the HDD literature and is still largely applied both by field engineers and academic researchers.

However, the PTOS is still somehow conservative, and several extensions of this controller were proposed in order to improve its performance. In particular, in [12] an extra degree of freedom to the controller is given, providing two independent control parameters in the design, and the works in [13] and [14] improve the controller performance via a damping scheduling scheme. While these controllers extend the PTOS improving on its performance, none of them are able to eliminate either the conservative variable (the so-called acceleration discount factor) or the switching function present in the PTOS.

A different approach toward tracking performance improvement was presented by Lin *et al.* [15], and came to be called composite nonlinear feedback (CNF) control. Such controllers are divided into two parts, a linear feedback law that is used to

Manuscript received February 9, 2011; accepted April 23, 2011. Date of publication June 23, 2011; date of current version August 24, 2012. Recommended by Technical Editor H. Ding. This work was supported in part by the Australian Research Councils Center of Excellence for Complex Dynamic Systems and Control, in part by the National Natural Science Foundation of China under Grant 91023034, and in part by the DMET Open Research Foundation under Grant DMETKF2010001.

A. T. Salton is with the School of Electrical Engineering and Computer Science, University of Newcastle, Callaghan, NSW 2308, Australia, and also with the Pontifícia Universidade Católica do Rio Grande do Sul, Porto Alegre 90619-900, Brazil (e-mail: aurelio.salton@uon.edu.au).

Z. Chen is with the School of Electrical Engineering and Computer Science, University of Newcastle, Callaghan, NSW 2308, Australia, and also with the State Key Laboratory of Digital Manufacturing Equipment and Technology, Huazhong University of Science and Technology, Wuhan 430074, China (e-mail: zhiyong.chen@newcastle.edu.au).

M. Fu is with the School of Electrical Engineering and Computer Science, University of Newcastle, Callaghan, NSW 2308, Australia, and also with the Department of Control Science and Engineering, Zhejiang University, Hangzhou 310058 China (e-mail: minyue.fu@newcastle.edu.au).

Digital Object Identifier 10.1109/TMECH.2011.2158110

stabilize the system with a low damping ratio, providing it with a fast rise time and a nonlinear feedback law that is designed such that the system becomes highly damped as the output approaches the reference point. The CNF was further expanded to multivariable linear systems in [16], and a complete and detail work on this technique may be found in [17]. One of the features of the CNF technique is that it takes into account the input saturation of the controller only during the stability analysis, not during the design itself. As a consequence, its performance is somewhat dependent on the tuning process: in order to approximate time-optimal performance, a different set of control parameters must be used for a different step size. To overcome this problem, different methods of automatic tuning have been proposed, such as the one in [18].

Needless to say, there are other control methods that achieve a good performance for this class of systems. These include the LQG approach [19], nonlinear PID control methods [20], sliding mode controllers [21], and model predictive control [22], among many others. Some of which do consider saturation and others do not.

It is our objective, however, to design a continuous controller that takes into account the saturation of the input, which is not computationally demanding and whose tuning is not step dependent. To achieve the aforementioned controller, we will propose two different approaches: 1) a controller that unifies the ideas by Workman and Lin and provides the system with a form of dynamic damping that is able to practically eliminate the conservatism present in the PTOS (the so-called acceleration discount factor), without the presence of overshoot; and 2) a purely nonlinear but also nonswitching controller that achieves near-time-optimal performance. Experimental results will show that a significant performance improvement results from the proposed designs.

The rest of the paper is organized as follows. Section II will present the model, introduce the PTOS in the perspective used in this paper, and briefly comment on a disturbance observer that is used to fit a larger class of systems to the rigid-body dynamics model. Section III will present a lemma used to prove the stability of the controllers. Sections IV and V will each present one different controller. Section VI will present experimental results and a short discussion, followed by concluding remarks given in Section VII.

II. PRELIMINARIES

This section will be used to introduce the system and present a brief discussion on the structure of controllers that approximate time-optimal performance. Also, because friction is an undesired but frequent phenomenon, a friction compensator will be referenced to so that a larger class of plants may be fitted in the rigid-body equations of motion used in this paper. It must be stressed, however, that none of these issues are the main purpose of this paper and the current discussion will be necessarily brief; so, we do not deviate from our main objective. The interested reader will be referred to the relevant literature.

A. Rigid-Body Dynamics Model

The system under initial consideration is given by a body of mass M with friction f and some unknown disturbance d

$$M\ddot{y} = \tilde{u} - f - d.$$

Friction compensation is still an active topic of research for robust tracking [23]. Here, we will make use of a well-established and successfully employed compensator that minimizes the effects of friction and disturbance (see [8] and [24], or [25], for further details); the system may be modeled by the rigid-body equations of motion given by

$$\begin{aligned} \dot{x}_1 &= x_2 \\ \dot{x}_2 &= b \text{ sat} \\ (u)y &= x_1 \end{aligned} \quad (1)$$

where x_1 and x_2 refer to the position and velocity, respectively, $b := 1/M$, and "sat" is the saturation block defined as

$$\text{sat}(z) = \begin{cases} \bar{u}, & z > \bar{u} \\ z, & |z| < \bar{u} \\ -\bar{u}, & z < -\bar{u} \end{cases} \quad (2)$$

with \bar{u} being the saturation level of the control input.

Most of the work in time-optimal performance was created for the rigid-body equations of motion described by system (1). In particular, it is for this system that the PTOS adapted the time-optimal control in order to achieve high performance in a practical controller. In what follows, a brief comment will be made on the construction of the PTOS, for it provides valuable background for understanding of the main contribution of this paper.

B. On the Construction of a Proximate Time-Optimal Controller

As previously mentioned, time-optimal performance for rigid-body dynamics systems is achieved by the bang-bang controller, a switching controller that applies maximal acceleration followed by maximal deceleration [1]. This control strategy may be described in a feedback structure by a switching curve given by

$$\begin{aligned} u_{to}(t) &= \text{sgn}(\sqrt{2b\bar{u}}|e| - v) \\ e &:= x_1 - y_r \\ v &:= x_2 \end{aligned} \quad (3)$$

where the $\text{sgn}(\cdot)$ function is defined as

$$\text{sgn}(z) = \begin{cases} \bar{u}, & z > 0 \\ 0, & z = 0 \\ -\bar{u}, & z < 0. \end{cases} \quad (4)$$

Workman transformed the TOC law (3) in a practical controller by accommodating measurement noise and plant uncertainties. For the purpose of this paper, his PTOS design may be described in the following three different steps.

Step 1: The effects of chattering are minimized by eliminating the $\text{sgn}(\cdot)$ function (4) where possible; also, a free parameter k

is applied in order to scale the control input

$$u(t) = k(-f(e) - v)$$

where $f(e)$ is defined as

$$f(e) = \text{sgn}(e)\sqrt{2b\bar{u}|e|}.$$

This control law is, in fact, a high gain that saturates the controller and drives the system to the time-optimal switching curve $v = -f(e)$, i.e., full acceleration is achieved. However, when the system reaches the switching curve, the control input goes to zero. Another term must be added so that the input goes from one saturation level to another (from \bar{u} to $-\bar{u}$ or vice versa).

Step 2: Saturation of the controller during deceleration is achieved by adding the term $\text{sgn}(e)\bar{u}$ from the controller

$$u(t) = k(-f(e) - v) + \text{sgn}(e)\bar{u}$$

or, in a more familiar form

$$u(t) = \text{sat}[k(-f_{\text{pto}}(e) - v)]$$

with $f_{\text{pto}}(e)$ defined as

$$f_{\text{pto}}(e) = \text{sgn}(e)(\sqrt{2b\bar{u}|e|} - \bar{u}/k). \quad (5)$$

While this controller is able to saturate the system both during acceleration and deceleration, it is not able to asymptotically track the reference. In fact, the equilibrium point is given by

$$\dot{y} = \dot{v} = 0 \quad \rightarrow \quad u = v = 0 \quad \rightarrow \quad f(e) = 0 \quad (6)$$

which implies

$$|e| = \frac{\bar{u}}{2bk^2}.$$

Step 3: Traditionally, asymptotic stability is achieved by implementing a switching control law. As the system approaches the reference, the controller switches from the complex nonlinear function (5) to a simple proportional derivative (PD) controller. The cost of using such a nonaggressive linear control law is that the PD controller is unable to prevent the system from overshooting. To overcome this problem, the so-called acceleration discount factor α was included in the original nonlinear function $f_{\text{pto}}(e)$, adding conservatism to the solution.

The control law becomes

$$u(t) = k_2(-f_{\text{ptos}}(e) - v) \quad (7)$$

with

$$f_{\text{ptos}}(e) = \begin{cases} (k_1/k_2)e, & \text{for } |e| \leq y_l \\ \text{sgn}(e)(\sqrt{2b\alpha\bar{u}|e|} - \bar{u}/k_2), & \text{for } |e| > y_l. \end{cases} \quad (8)$$

A stability condition requires that $0 < \alpha < 1$, and the following constraints guarantee a continuous switching of the controller:

$$y_l = \frac{\bar{u}}{k_1} \quad k_2 = \sqrt{\frac{2k_1}{b\alpha}}. \quad (9)$$

Notice that this discussion only scratches the surface of the PTOS; for full details, the reader should refer to the references presented in Section I.

The main objective of this paper will be to improve the performance of this controller by eliminating the necessity for the

discount acceleration factor α . While theoretically α could take values arbitrarily close to 1, in practice, it typically ranges from $0.5 < \alpha < 0.8$ in order to prevent the system from overshooting. We will achieve $\alpha \rightarrow 1$ via two different methods.

In the first method, we use an aggressive control law applied the system enters the region $|e| \leq y_l$ in (8). Instead of switching to the simple PD controller, equation (8) will switch to a form of the CNF such that damping is added to the system as the output approaches the reference. This results in a response with no or limited overshoot, while pushing $\alpha \rightarrow 1$. Notice that the tuning problems associated with the CNF will be minimal because this controller will only be used in a very small range, namely $|e| \leq y_l$. The design of this control law will be given in Section IV. The second method, to be detailed in Section V, will use a nonlinear controller that does not require any switching and achieves asymptotic stability with $\alpha = 1$.

Without loss of generality, we assume $y_r = 0$, and the problem reduces to a stabilization problem of the equilibrium point $x := [x_1, x_2]^T = 0$. We will start with a stability result that may be applied to both the controllers and, then, move on to exposing them individually.

III. STABILITY LEMMA

The following is a result on stability that will be used by the controllers designed in the next sections.

Lemma 3.1: Consider the closed-loop system composed of (1) and the control law

$$u = -h_1(x_1) - h_2(x_1)x_2 \quad (10)$$

where $h_1(\cdot)$ and $h_2(\cdot)$ are the piecewise continuously differentiable functions with $h_1(0) = 0$. Suppose the following conditions¹ are satisfied for $x_1 \in \mathbb{T}$ with \mathbb{T} being a subset of \mathbb{R} :

- A1: $h_1'(x_1) > 0$ and $\lim_{x_1 \rightarrow \pm\infty} h_1(x_1) = \pm\infty$;
- A2: $0 < h_2(x_1)$;
- A3: $\bar{u}(h_1' - h_2^2b) + h_2'(\bar{u} - h_1)^2/h_2 < h_1'h_1 < \bar{u}(bh_2^2 - h_1') + h_2'(\bar{u} + h_1)^2/h_2$.

Then, the trajectory $x(t)$ of the closed-loop system satisfies $\lim_{t \rightarrow \infty} x(t) = 0$ if $x_1(t) \in \mathbb{T}, \forall t \geq 0$.

Proof: The proof will be divided into three parts showing that 1) given an unsaturated region \mathbb{U} defined by

$$\mathbb{U} = \{(x_1, x_2) \in \mathbb{R}^2 \mid | -h_1(x_1) - h_2(x_1)x_2 | \leq \bar{u}\}$$

any trajectory starting outside \mathbb{U} enters \mathbb{U} in a finite time; 2) any trajectory in \mathbb{U} remains there indefinitely; and 3) once in \mathbb{U} , the trajectory converges to the equilibrium point, i.e., $\lim_{t \rightarrow \infty} x(t) = 0$.

1) Suppose a given initial condition $(x_1(0), x_2(0))$ belongs to the region outside \mathbb{U} , where $u(0) > \bar{u}$, i.e.,

$$u(0) = -h_1(x_1(0)) - h_2(x_1(0))x_2(0) > \bar{u}.$$

It must be shown that for a finite time $T > 0$, the input will be such that $u(T) = \bar{u}$. From the system equations (1), the

¹We define $h_i'(x_1) := dh_i(x_1)/dx_1$ as the derivative of h_i . Since $h_i(\cdot)$ is piecewise continuously differentiable, at the discontinuous point, h_i has different left and right derivatives. We assume that A1 and A3 are satisfied for both derivatives. We drop the dependence of the functions on x_1 for the ease of notation if it does not cause any confusion.

evolution of the system will be

$$\begin{aligned}x_2(t) &= b\bar{u}t + x_2(0) > 0 \\x_1(t) &= b\bar{u}t^2/2 + x_2(0)t + x_1(0) > 0\end{aligned}$$

for a sufficiently large t . From assumptions A1 and A2, we have $h_2(x_1(t))x_2(t) > 0$, and hence

$$\begin{aligned}u(t) &= -h_1(x_1(t)) - h_2(x_1(t))x_2(t) \\&< -h_1(b\bar{u}t^2/2 + x_2(0)t + x_1(0)).\end{aligned}$$

Therefore, $u(t)$ satisfies $\lim_{t \rightarrow \infty} u(t) = -\infty$, and due to the continuity of $h_i(\cdot)$, it must be that $u(t)$ takes all the values in the interval $[u(0), -\infty)$. This implies that for a finite time $T > 0$, $u(T) = \bar{u}$, i.e., the system enters \mathbb{U} . By symmetry, the same is true for trajectories satisfying $u(0) < -\bar{u}$.

2) In order to prove that any trajectory starting in \mathbb{U} will remain there indefinitely, let T denote the time when the trajectories are at the boundary of \mathbb{U} , i.e., $|u(T)| = \bar{u}$. These trajectories will stay in \mathbb{U} if

$$u(T)\dot{u}(T) < 0 \quad (11)$$

where $\dot{u} = -(h'_1(x_1)\dot{x}_1 + h_2(x_1)\dot{x}_2 + h'_2(x_1)\dot{x}_1x_2)$ is the change rate of u , because either $u(T) = \bar{u}$ and $\dot{u} < 0$, or $u(T) = -\bar{u}$ and $\dot{u} > 0$. We consider the case when $u(T) = \bar{u}$. Then

$$\begin{aligned}\dot{u} &= -(h'_1x_2 + h_2b\bar{u} + h'_2x_2^2) \\&= h'_1\left(\frac{\bar{u} + h_1}{h_2}\right) - h_2b\bar{u} - h'_2\left(\frac{\bar{u} + h_1}{h_2}\right)^2 \\&= \frac{h'_1h_1}{h_2} + \frac{h'_1\bar{u}}{h_2} - h_2b\bar{u} - h'_2\left(\frac{\bar{u} + h_1}{h_2}\right)^2 < 0\end{aligned} \quad (12)$$

is guaranteed by assumption A3. Next, we consider the case when $u(T) = -\bar{u}$, and then, a similar calculation shows that

$$\dot{u} = \frac{h'_1h_1}{h_2} - \frac{h'_1\bar{u}}{h_2} + h_2b\bar{u} - h'_2\left(\frac{\bar{u} - h_1}{h_2}\right)^2 > 0 \quad (13)$$

is also guaranteed by assumption A3.

3) We may now proceed to the stability proof of the system when inside the region \mathbb{U} and neglect the effects of saturation. To do so, let us take the following as a Lyapunov function candidate:

$$V(x) = \int_0^{x_1} h_1(y)dy + \frac{x_2^2}{2b} \quad (14)$$

which is positive definite and radially unbounded.

Along the trajectory of the closed-loop system inside the region \mathbb{U} , we have

$$\begin{aligned}\dot{V}(x) &= h_1(x_1)x_2 - x_2[h_1(x_1) + h_2(x_1)x_2] \\&= -h_2(x_1)x_2^2 \leq 0.\end{aligned}$$

It remains to show that $\dot{V}(x) = 0$ only at the origin

$$\dot{V}(x) = 0 \Rightarrow h_2(x_1)x_2^2 = 0 \Rightarrow x_2 = 0.$$

This in turn implies that

$$x_2(t) = 0 \Rightarrow \dot{x}_2(t) = 0 \Rightarrow h_1(x_1(t)) = 0 \Rightarrow x_1(t) = 0.$$

We may now claim LaSalle's invariance principle and assert that $\lim_{t \rightarrow \infty} x(t) = 0$. This completes the proof. \square

This result provides us with a great deal of liberty when designing a controller for system (1) because both $h_1(\cdot)$ and $h_2(\cdot)$ may be nonlinear functions. We will take advantage of this liberty in design and of the simplicity of the equations describing the system in order to reach time-optimal performance.

IV. DYNAMICALLY DAMPED PTOS

In this section, we will adapt control law (7) and present an alternative controller to be applied when the system enters the region $|e| \leq y_l$. It will be shown that this will generate an improved performance inasmuch as an aggressive controller in that region allows us to be less conservative when $|e| > y_l$.

A. Controller Design

Referring to (7), one notices that while $|e| \leq y_l$, the linear gain $K = [k_1 \ k_2]$ may be parameterized as

$$K = [4\pi^2\omega^2 \ 4\pi\omega\zeta]$$

with ω representing the undamped natural frequency of the system and ζ the damping ratio. As pointed out in [13], the continuity conditions on the PTOS limit the damping ratio of the system. In fact, from (9)

$$\zeta = \sqrt{\frac{1}{2\alpha}}$$

and it is evident that the larger the α , the smaller the damping and, consequently, the larger the overshoot. For example, if α is pushed to its limit, i.e., $\alpha = 1$, then $\zeta = 0.707$ resulting in a large overshoot. However, by making use of a dynamic gain when $|e| \leq y_l$, we can add damping to the system via a nonlinear feedback following the ideas of Lin *et al.* in [15]. As opposed to the ideas of [13], the proposed controller will use a dynamic damping scheme only at $|e| \leq y_l$. This will allow the system to avoid overshooting while retaining a high performance ($\alpha \rightarrow 1$) and the simplicity of the PTOS. This controller is presented in the next theorem. Notice that for $|x_1| > y_l$, the traditional PTOS is applied, but for $|x_1| \leq y_l$, a dynamic gain is applied to the velocity feedback in order to add damping.

Theorem 4.1: Consider the closed-loop system composed of (1) and (10) with

$$h_1(x_1) = \begin{cases} k_1x_1, & |x_1| \leq y_l \\ \text{sgn}(x_1)k_2\left(\sqrt{2b\bar{u}\alpha|x_1|} - \bar{u}/k_2\right), & |x_1| > y_l \end{cases}$$

$$h_2(x_1) = k_2(1 + \rho(x_1))$$

$$\rho(x_1) = \begin{cases} \beta(|x_1| - y_l)^2, & |x_1| \leq y_l \\ 0, & |x_1| > y_l \end{cases}$$

where

$$k_1 > 0, \quad k_2 = \sqrt{\frac{2k_1}{b\alpha}}, \quad y_l = \frac{\bar{u}}{k_1} \quad (15)$$

and

$$0 < \alpha < 1, \quad (\alpha^{-1} - 1)/(4y_l^2) > \beta \geq 0. \quad (16)$$

Then, the closed-loop system is globally asymptotically stable in the sense that $\lim_{t \rightarrow \infty} x(t) = 0$ for any $x(0) \in \mathbb{R}^2$.

Proof: The proof will be based on Lemma 3.1 with $\mathbb{T} = \mathbb{R}$. In particular, we need to examine the three assumptions A1–A3.

Clearly, $h_1(\cdot)$ is an odd function with

$$h_1(x_1) = -h_1(-x_1), \quad \lim_{x_1 \rightarrow \pm\infty} h_1(x_1) = \pm\infty. \quad (17)$$

Its derivative satisfies $h_1'(x_1) = h_1'(-x_1)$. So, it suffices to show that $h_1'(x_1) > 0 \forall x_1 \geq 0$ for A1. Actually, we have $h_1'(x_1) = k_1 > 0$ for $x_1 < y_l$ and $h_1'(x_1) = k_2 \sqrt{b\bar{u}\alpha/(2x_1)} > 0$ for $x_1 > y_l$. With the parameters given in (15), it is easy to see that, when $x_1 = y_l$, we have

$$k_1 x_1 = \text{sgn}(x_1) k_2 \left(\sqrt{2b\bar{u}\alpha|x_1|} - \frac{\bar{u}}{k_2} \right)$$

and

$$k_1 = k_2 \sqrt{b\bar{u}\alpha/(2x_1)}$$

which imply that $h_1(\cdot)$ is continuous and continuously differentiable, respectively. So, we have $h_1'(y_l) = k_1 > 0$. Assumption A1 is, thus, satisfied.

Assumption A2 is clearly true because $h_2(x_1) \geq k_2 > 0$.

We will consider two cases for assumption A3.

Case 1: $|x_1| \leq y_l$. First, we note that the function $h_2(x_1)$ is an even piecewise continuously differentiable with $h_2(x_1) = h_2(-x_1)$ and $h_2'(x_1) = -h_2'(-x_1)$. Moreover

$$\begin{aligned} h_2'(x_1) &= 2k_2\beta(x_1 - y_l) \leq 0, \quad x_1 > 0 \\ h_2'(0^+) &= -h_2'(0^-) = 2k_2\beta(-y_l) \leq 0. \end{aligned}$$

In this case, A3 becomes

$$\begin{aligned} \bar{u}(k_1 - h_2^2 b) + h_2'(\bar{u} - h_1)^2/h_2 &< k_1^2 x_1 < \bar{u}(bh_2^2 - k_1) \\ &+ h_2'(\bar{u} + h_1)^2/h_2. \end{aligned}$$

When $x_1 > 0$, since $bh_2^2 - k_1 \geq bk_2^2 - k_1 > 0$, and $h_2'(x_1) \leq 0$, it suffices to show

$$k_1^2 x_1 < \bar{u}(bh_2^2 - k_1) + h_2'(\bar{u} + h_1)^2/h_2 \quad (18)$$

or

$$k_1^2 y_l + \bar{u}k_1 < \bar{u}bh_2^2 + h_2'(\bar{u} + h_1)^2/h_2.$$

It is true from the following calculation:

$$\begin{aligned} \bar{u}bh_2^2 + h_2'(\bar{u} + h_1)^2/h_2 &\geq \bar{u}bk_2^2 + (2k_2\beta(x_1 - y_l))(\bar{u} + h_1)^2/k_2 \\ &\geq \bar{u}bk_2^2 - (2k_2\beta y_l)(\bar{u} + h_1)^2/k_2 \\ &\geq \bar{u}bk_2^2 - (2k_2\beta y_l)(\bar{u} + k_1 y_l)^2/k_2 > k_1^2 y_l + \bar{u}k_1 \end{aligned}$$

where the last inequality is equivalent to (16).

When $x_1 < 0$, since $bh_2^2 - k_1 > 0$, and $h_2'(x_1) > 0$, it suffices to show

$$\bar{u}(k_1 - h_2^2 b) + h_2'(\bar{u} - h_1)^2/h_2 < k_1^2 x_1$$

which is true following the same argument.

When $x_1 = 0$, it suffices to show

$$\bar{u}(bh_2^2(0) - k_1) > |h_2'(0)|\bar{u}^2/h_2(0)$$

TABLE 1
PARAMETERS OF PTOS AND DDPTOS

Parameter	Traditional	Proposed
k_1	2.09	2.09
k_2	0.019	0.016
α	0.7	0.99
β	-	0.02

which is in the form of (18) with $x_1 = 0$, and the remaining proof follows.

Case 2: $|x_1| > y_l$. In this case, A3 becomes

$$\bar{u}(h_1' - k_2^2 b) < h_1' h_1 < \bar{u}(bk_2^2 - h_1').$$

By symmetry, it suffices to show

$$h_1' h_1 < \bar{u}(bk_2^2 - h_1'), \quad x_1 > y_l$$

that is

$$\begin{aligned} (k_2 \sqrt{b\bar{u}\alpha/(2x_1)})(k_2(\sqrt{2b\bar{u}\alpha x_1} - \bar{u}/k_2)) \\ < \bar{u}(bk_2^2 - k_2 \sqrt{b\bar{u}\alpha/(2x_1)}), \quad x_1 > y_l. \end{aligned}$$

Some simple calculation shows that this inequality reduces to $\alpha < 1$. The proof is, thus, complete. \square

Remark 4.1: By choosing $\beta = 0$, the proposed controller becomes identical to the PTOS. There is, however, a severe loss in performance when no dynamic damping is added to the controller inasmuch as the acceleration discount factor α must take values considerably smaller than 1; so, the system is able to achieve acceptable levels of overshoot. In summary, the dynamic damping allows the controller to be more aggressive when $|x_1| \leq y_l$, which in turn allows the controller to be less conservative ($\alpha \rightarrow 1$), when $|x_1| > y_l$, generating an improved performance during the overall trajectory.

B. Simulation Results

Surely, we expect the proposed controller to have some improvement over the traditional one; this will be demonstrated in this section. In order to see how significant the performance improvement is, we will also compare both the controllers to the TOC.

Here, the parameters are the same as those of the real system that will be used to implement these controllers in Section VI. The system is as in (1) with $\bar{u} = 1$ and $b = 17\,000$ so that x_1 units are given in millimeters. The time-optimal control is applied via the simple equation in (3). The parameters used in both the traditional PTOS and the dynamically damped proposed controller are given in Table I. Notice that the main difference in parameters comes from the acceleration discount factor α , because the velocity gain k_2 only changes as a result of the continuity conditions (9) and (15). Finally, it is important to realize that this single set of parameters was used for all responses. This shows how easy this is to tune these controllers once the tuning is not dependent on the step size.

Fig. 1 shows the normalized response y/y_r for steps of 1, 10, 25, 50, and 70 mm. Notice how closer to the time-optimal performance the proposed controller is when compared to the

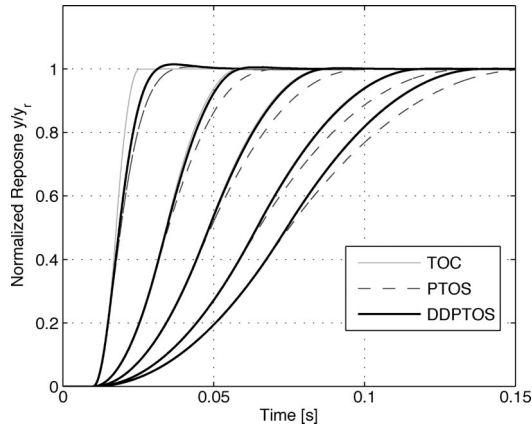


Fig. 1. Normalized simulated responses (y/y_r) for steps of 1, 10, 25, 50, and 70 mm for the three comparative controllers.

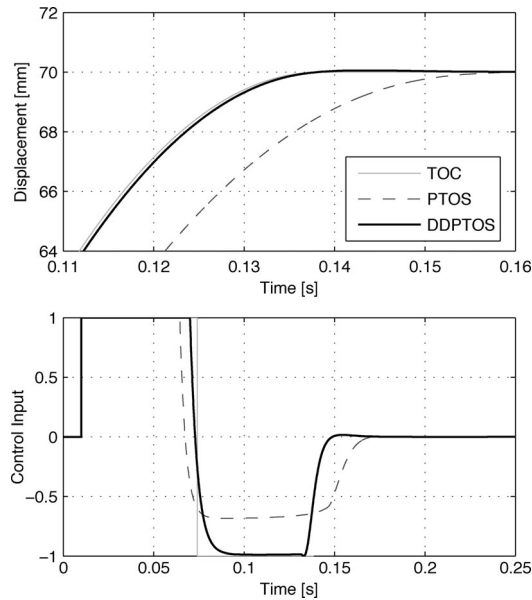


Fig. 2. Simulated response of TOC, PTOS, and DDPTOS for a 70-mm step reference.

traditional PTOS. This is even clearer in Fig. 4, where we have zoomed in at the 70 mm response on the top plot and we show the three different inputs in the bottom plot. As expected, the acceleration profile of all three controllers is very similar because at the beginning of the trajectories all of them are saturated. However, the dynamically damped (DDPTOS) input is much closer to that of TOC on the rest of the trajectory. Because the proposed controller is more aggressive during deceleration, it is able to maintain the input saturated for a longer time during acceleration, which generates the performance improvement shown in the plots.

V. QUASI-TIME-OPTIMAL SERVOMECHANISM

It was argued in Section IV that the PTOS design had to be somehow conservative because of the simple PD controller applied when the system approaches the reference point. We then proceeded by proposing a different controller such that the

conservatism due to the switching control law was minimized. In this section, we will improve the system performance via a different approach, i.e., a nonswitching controller will be proposed such that no conservatism is added to the system. In fact, the acceleration discount factor is unnecessary in this control strategy ($\alpha = 1$). Furthermore, the controller itself is of simpler structure, once there is no switching between different control laws. Finally, there are only two parameters to be tuned, and it will be shown that the same set of parameters may be applied for a wide range of steps while retaining near-optimal performance.

A. Controller Design

From the discussion in Section II, Step 2, we recall that the necessity of a switching control law is due to asymptotic stability of the system, i.e., function (5) provides the system with an equilibrium point away from the origin. Therefore, it is only logical to investigate other types of controllers that satisfy the stability criteria in Section III without the necessity of switching functions. Based on the previous discussion, a nonswitching controller that achieves near-time-optimal performance is proposed in the following theorem.

Theorem 5.1: Consider the closed-loop system composed of (1) and (10), with

$$\begin{aligned} h_1(x_1) &= k_1 \operatorname{sgn}(x_1) \left(\sqrt{2b\bar{u}\psi(x_1)|x_1|} - (\bar{u}/k_1)\psi(x_1) \right) \\ h_2(x_1) &= k_2 \\ \psi(x_1) &= (1 - e^{-\mu|x_1|}) \end{aligned} \quad (19)$$

for any

$$k_1 > 0, \quad 2k_1^2 b/\bar{u} > \mu > 0.$$

Then, the closed-loop system is semiglobally asymptotically stable in the sense that, for any compact set $\mathbb{X}_o \subset \mathbb{R}^2$, there exists a $k_2 > 0$ (depending on \mathbb{X}_o), such that any trajectory with $x(0) \in \mathbb{X}_o$ satisfies $\lim_{t \rightarrow \infty} x(t) = 0$.

Proof: First, we note that the function $h_1(\cdot)$ has the following properties. It is a continuously differentiable odd function with

$$h_1(x_1) = -h_1(-x_1), \quad \lim_{x_1 \rightarrow \pm\infty} h_1(x_1) = \pm\infty. \quad (20)$$

Its derivative satisfies $h_1'(x_1) = h_1'(-x_1)$,

$$\begin{aligned} h_1'(x_1) &= k_1 \sqrt{b\bar{u}/2} \left(\frac{\psi(x_1) + x_1\psi'(x_1)}{\sqrt{x_1\psi(x_1)}} \right) - \bar{u}\psi'(x_1) \\ &= k_1 \sqrt{\frac{b\bar{u}\psi(x_1)}{2x_1}} + k_1 \sqrt{\frac{b\bar{u}x_1}{2\psi(x_1)}} \psi'(x_1) - \bar{u}\psi'(x_1) \\ &= k_1 \sqrt{\frac{b\bar{u}\psi(x_1)}{2x_1}} - \frac{\bar{u}}{2}\psi'(x_1) \\ &\quad + \left(k_1 \sqrt{\frac{b\bar{u}x_1}{2\psi(x_1)}} - \frac{\bar{u}}{2} \right) \psi'(x_1) > 0, \quad \forall x_1 > 0 \end{aligned} \quad (21)$$

and

$$\begin{aligned} h'_1(0) &= \lim_{x_1 \rightarrow 0} k_1 \sqrt{\frac{b\bar{u}\psi(x_1)}{2x_1}} + k_1 \sqrt{\frac{b\bar{u}x_1}{2\psi(x_1)}} \psi'(x_1) - \bar{u}\psi'(x_1) \\ &= k_1 \sqrt{\frac{b\bar{u}\mu}{2}} + k_1 \sqrt{\frac{b\bar{u}}{2\mu}} \mu - \bar{u}\mu = k_1 \sqrt{2b\bar{u}\mu} - \bar{u}\mu > 0. \end{aligned}$$

In the last inequality of (21), we use the following facts.

1) The inequality $|x_1|/\psi(x_1) \geq 1/\mu$ implies

$$k_1 \sqrt{\frac{b\bar{u}x_1}{2\psi(x_1)}} \geq k_1 \sqrt{\frac{b\bar{u}}{2\mu}} > \frac{\bar{u}}{2}.$$

2) The inequality

$$k_1 \sqrt{\frac{b\bar{u}\psi(x_1)}{2x_1}} > \frac{\bar{u}}{2} \psi'(x_1)$$

is equivalent to

$$\frac{2k_1^2 b}{\bar{u}} > \frac{\psi'^2(x_1)x_1}{\psi(x_1)}$$

which holds if

$$\mu \geq \frac{\psi'^2(x_1)x_1}{\psi(x_1)}$$

or

$$\bar{h}(x_1) := 1 - e^{-\mu x_1} - \mu e^{-2\mu x_1} x_1 \geq 0.$$

It is true because $\bar{h}(0) = 0$ and

$$\bar{h}'(x_1) = \mu e^{-\mu x_1} - \mu e^{-2\mu x_1} + 2\mu^2 e^{-2\mu x_1} x_1 \geq 0.$$

The remaining proof of this theorem is based on Lemma 3.1. To this end, we need to define a subset $\mathbb{T} \subset \mathbb{R}$. We first show that there exists a finite time T such that

$$x(T) \in \mathbb{U}, \quad |x_1(t)| \leq \bar{x}_1, \quad |x_2(t)| \leq \bar{x}_2 \quad \forall t \in [0, T] \quad (22)$$

for some constants \bar{x}_1 and \bar{x}_2 depending on \mathbb{X}_o . If $x(0) \in \mathbb{U}$, (22) is trivial with $T = 0$. Otherwise, the proof relies on the same argument used in item 1 of the proof of Lemma 3.1. In particular, we note that, for $x(0) \in \mathbb{X}_o$ and a finite T , $\|x(t)\|$ is bounded for $t \in [0, T]$. Then, we can define a finite constant $x_1^* > 0$ as

$$\int_0^{x_1^*} h_1(y) dy = V([\bar{x}_1, \bar{x}_2]) = \int_0^{\bar{x}_1} h_1(y) dy + \frac{\bar{x}_2^2}{2b} \quad (23)$$

and, hence, $\mathbb{T} = \{x \in \mathbb{R} \mid |x| \leq x_1^*\}$. Clearly, we have $x_1^* \geq \bar{x}_1$.

It is ready to check assumptions A1–A3 in Lemma 3.1. In fact, A1 is satisfied from the aforementioned properties of $h_1(\cdot)$ and A2 is self-evident. It remains to examine A_3 , i.e.

$$\bar{u}(h'_1(x_1) - bk_2^2) < h'_1(x_1)h_1(x_1) < \bar{u}(bk_2^2 - h'_1(x_1)).$$

Due to the symmetry, it suffices to show

$$h'_1(x_1)h_1(x_1) < \bar{u}(bk_2^2 - h'_1(x_1)) \quad \forall x_1^* \geq x_1 \geq 0.$$

It is true if k_2 is sufficiently large for

$$k_2^2 > h'_1(x_1)h_1(x_1)/(\bar{u}b) + h'_1(x_1)/b \quad \forall x_1^* \geq x_1 \geq 0.$$

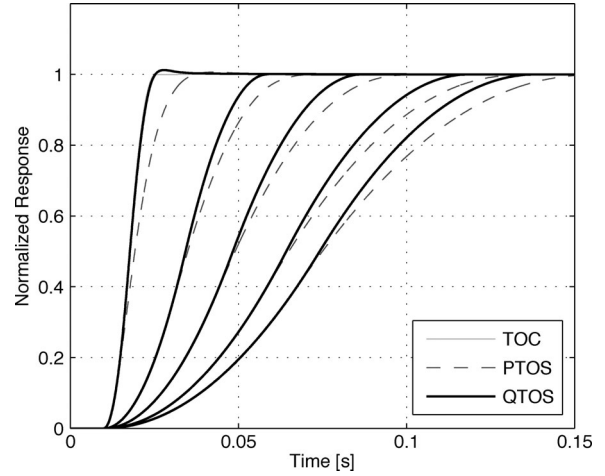


Fig. 3. Normalized simulated responses (y/y_r) for steps of 1, 10, 25, 50, and 70 mm for the three comparative controllers.

It should be noted that $x_1^* \geq x_1$ is critical in the aforementioned inequality. Actually, the term on the right-hand side approaches infinity as x_1 goes to infinity; so, it is impossible to find a finite k_2 for the inequality for all $x_1 \geq 0$. Now, A_3 is satisfied.

What left is to show that $x_1(t) \in \mathbb{T} \forall t \geq 0$. From the aforementioned definition of \mathbb{T} , $x_1(t) \in \mathbb{T}$ is true for $t \in [0, T]$ as shown in (22). For any $t > T$, the trajectory is inside \mathbb{U} , we have $\dot{V}(x) < 0$ from item 3) of the proof of Lemma 3.1, i.e.

$$\begin{aligned} \int_0^{x_1(t)} h_1(y) dy &\leq \int_0^{x_1(T)} h_1(y) dy + \frac{x_2(t)^2}{2b} \\ &= V(x(t)) < V(x(T)). \end{aligned}$$

On the other hand, (22) implies

$$|x_1(T)| \leq \bar{x}_1, \quad |x_2(T)| \leq \bar{x}_2$$

and, hence,

$$V(x(T)) \leq \int_0^{\bar{x}_1} h_1(y) dy + \frac{\bar{x}_2^2}{2b} = \int_0^{x_1^*} h_1(y) dy.$$

As a result, we have

$$\int_0^{x_1(t)} h_1(y) dy \leq \int_0^{x_1^*} h_1(y) dy$$

or $|x_1(t)| \leq x_1^*$, i.e., $x_1(t) \in \mathbb{T}$. The proof is, thus, complete. \square

B. Simulation Results

Here, we will perform the same comparison that we have performed in Section IV-B. The PTOS parameters are the same given in Table I, and the quasi-TOS (QTOS) parameters are

$$k_1 = k_2 = 0.325, \quad \mu = 36. \quad (24)$$

Fig. 3 shows the normalized response y/y_r for steps of 1, 10, 25, 50, and 70 mm as in Section IV-B. Once again the proposed controller is much closer to the time-optimal performance than the traditional PTOS. This is also clear in Fig. 4, where we focused at the 70 mm response. The top plot shows the trajectories of the

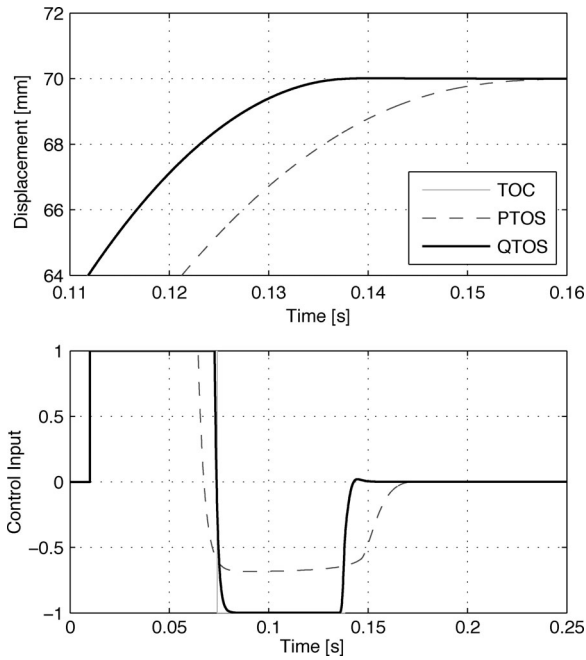


Fig. 4. Simulated response of TOC, PTOS, and QTOS for a 70-mm step reference.

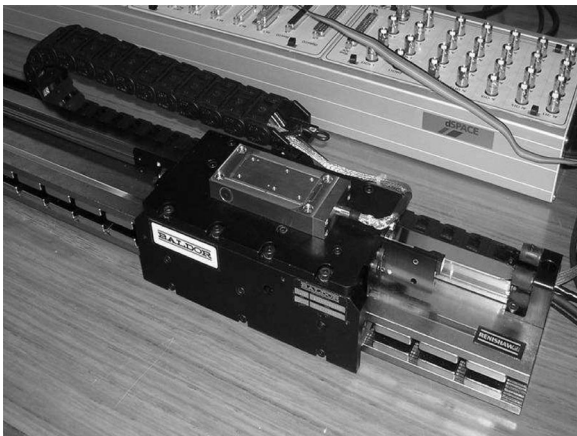


Fig. 5. Experimental setup of the electromagnetic motor.

position and the bottom plot shows the three different inputs. The proposed QTOS input is much closer to that of TOC providing the system with an aggressive performance, very similar to that achieved by TOC.

VI. EXPERIMENTAL RESULTS AND DISCUSSION

The proposed controllers, along with the traditional PTOS, were implemented in the linear motor (LM) set-up depicted in Fig. 5, whose parameters are $b = 1.7 \times 10^4$ and $\bar{u} = 1$. We have made use of a DSP system (dSPACE-DS1103) with a sampling frequency of 10 kHz and have limited the overshoot of all three controllers to 30 μm independent of the step size. Moreover, a conventional state observer was necessary once only the position is available for feedback. The controller parameters are the same as given in Sections IV-B and V-B. It is important to emphasize that for all the step responses, we have used the same set of

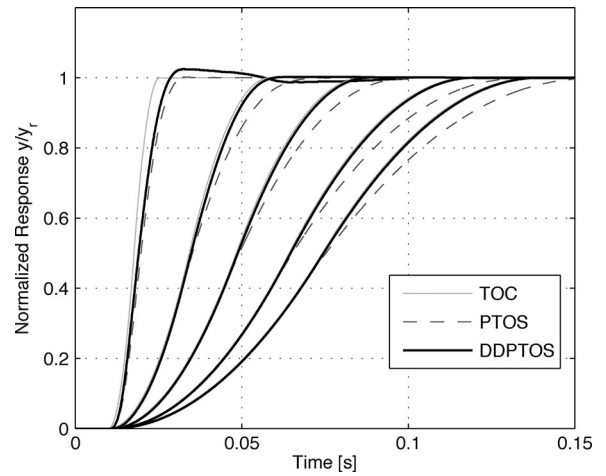


Fig. 6. Normalized plant responses (y/y_r) for steps of 1, 10, 25, 50, and 70 mm for the three compared controllers.

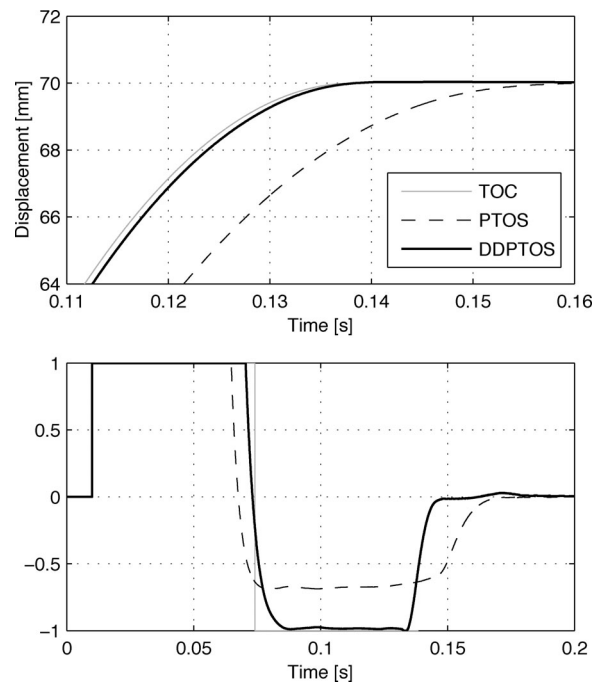


Fig. 7. Plant response of TOC, PTOS, and DDPTOS for a 70-mm step reference.

parameters. This shows how simple it is to tune the proposed controllers, both of which only have few parameters to be tuned, namely k_1 and β for the DDPTOS, and k_i and μ for the QTOS. We have also compared the plant responses to the simulated TOC response in order to show that, despite the tuning simplicity, the proposed controllers are able to achieve quasi-time-optimal performance.

Figs. 6 and 8 show the normalized responses for the step inputs of 1, 5, 10, 25, 50, and 70 mm. It is clear from the figures that the proposed controllers are considerably faster than the traditional one and closer to the time-optimal performance. This is also evident when analyzing the plots of Figs. 7 and 9, where the control inputs are also depicted. Particularly, notice how

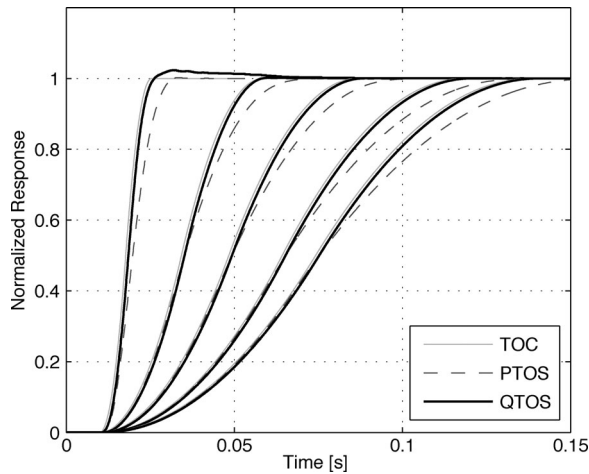


Fig. 8. Plant responses (y/y_r) for steps of 1, 10, 25, 50, and 70 mm.

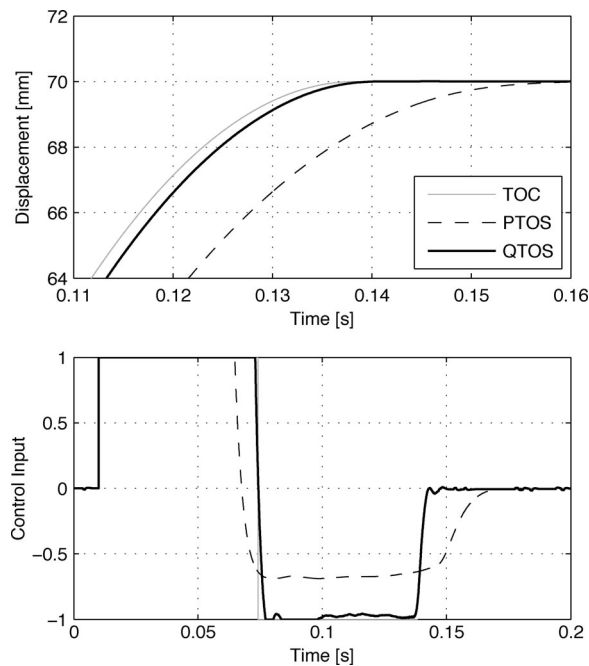


Fig. 9. Plant response of TOC, PTOS, and QTOS for a 70-mm step reference.

the proposed controllers approximate the time-optimal input. Evidently, this is only possible because we have dropped the conservatism generated by the acceleration discount factor α .

It remains to present some final discussion comparing the proposed controllers to each other, after all, despite presenting very similar performances, they are crucially different in some aspects. As opposed to the QTOS, the DDPTOS remains a switching control law. Surely, the conservatism once added to maintain the switching controller continuous was eliminated, but the switching function still increases the complexity of the controller. The advantage of maintaining such complexity is that some form of linear analysis may be performed to the controller inasmuch as the notions of natural frequency and (dynamic) damping continue to make sense when the trajectories approach the reference. On the other hand, the QTOS is a purely nonlin-

ear controller and linear analysis are not of the same usefulness. Nevertheless, its tuning process is also particularly easy, and because there is no switching involved, this controller is even simpler than the traditional PTOS. In summary, both controllers achieve a near-time-optimal performance, the DDPTOS does so allowing a simpler (linear) analysis, and the QTOS allowing a simpler implementation.

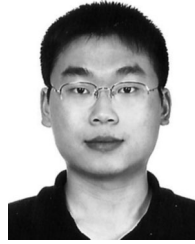
VII. CONCLUSION

This paper has proposed two different controllers that achieve near-time-optimal performance for electromagnetic systems described by the rigid-body equations of motion. The proposed designs expanded on the ideas of the traditional PTOS and improved this controller's performance by eliminating the conservatism present in it. The so-called acceleration discount factor was pushed to the boundary ($\alpha \rightarrow 1$) by the proposed DDPTOS and was completely eliminated by the QTOS. Both these controllers take full consideration of the saturation level of the control input; in fact, instead of avoiding saturation, they were specifically designed to saturate both at the acceleration and deceleration profiles. Furthermore, a good performance is achieved with simple tuning on the part of the designer: the near-time-optimal performance is not step dependent and one set of parameters performs well for a wide range of reference steps. Experimental results validated the proposed controllers by showing that their plant performance is comparable to the simulated TOC performance.

REFERENCES

- [1] A. E. Bryson and Y. C. Ho, *Applied Optimal Control*. New York: Hemisphere, 1975.
- [2] H. K. Khalil, *Nonlinear Systems*, 3rd ed. Upper Saddle River, NJ: Prentice-Hall, 2002.
- [3] H. Grabner, W. Amrhein, S. Silber, and W. Gruber, "Nonlinear feedback control of a bearingless brushless dc motor," *IEEE/ASME Trans. Mechatronics*, vol. 15, no. 1, pp. 40–47, Feb. 2010.
- [4] B. M. Chen, T. H. Lee, K. Peng, and V. Venkataramanan, *Hard Disk Drive Servo Systems*, 2nd ed. Secaucus, NJ: Springer-Verlag, 2006.
- [5] J. Zheng, M. Fu, Y. Wang, and C. Du, "Nonlinear tracking control for a hard disk drive dual-stage actuator system," *IEEE/ASME Trans. Mechatronics*, vol. 13, no. 5, pp. 510–518, Oct. 2008.
- [6] K. W. Chan, W. H. Liao, and I. Y. Shen, "Precision positioning of hard disk drives using piezoelectric actuators with passive damping," *IEEE/ASME Trans. Mechatronics*, vol. 13, no. 1, pp. 147–151, Feb. 2008.
- [7] J. Zheng, W. su, and M. Fu, "Dual-stage actuator control design using a doubly coprime factorization approach," *IEEE/ASME Trans. Mechatronics*, vol. 15, no. 3, pp. 339–348, Jun. 2010.
- [8] A. T. Salton, Z. Chen, J. Zheng, and M. Fu, "Preview control of dual-stage actuator systems for super fast transition time," *IEEE/ASME Trans. Mechatronics*, vol. 16, no. 4, pp. 758–763, Aug. 2011.
- [9] M. Workman, "Adaptive proximate time-optimal control servomechanisms," Ph.D. dissertation, Inf. Syst. Lab., Stanford University, Stanford, CA, 1987.
- [10] M. L. Workman, R. L. Kosut, and G. F. Franklin, "Adaptive proximate time-optimal servomechanisms—Continuous time case," in *Proc. 6th Amer. Control Conf.*, Minneapolis, MN, 1987, pp. 589–594.
- [11] A. M. Pascoal, R. L. Kosut, G. F. Franklin, D. R. Meldrum, and M. L. Workman, "Adaptive time-optimal control of flexible structures," in *Proc. 8th Amer. Control Conf.*, Pittsburgh, PA, 1989, pp. 19–24.
- [12] A. Dhanda and G. F. Franklin, "An improved 2-DOF proximate time optimal servomechanism," *IEEE Trans. Magn.*, vol. 45, no. 5, pp. 2151–2164, May 2009.
- [13] Y. M. Choi, J. Jeong, and D. G. Gweon, "A novel damping scheduling scheme for proximate time optimal servomechanism in hard disk drives," *IEEE Trans. Magn.*, vol. 42, no. 3, pp. 468–472, Mar. 2006.

- [14] Y. M. Choi, J. Jeong, and D. G. Gweon, "Modified damping scheduling scheme for proximate time optimal servomechanism for improvements in short strokes in hard disk drives," *IEEE Trans. Magn.*, vol. 44, no. 4, pp. 468–472, Apr. 2008.
- [15] Z. Lin, M. Pachter, and S. Banda, "Toward improvement of tracking performance-nonlinear feedback for linear systems," *Int. J. Control*, vol. 70, pp. 1–11, 1998.
- [16] M. C. Turner, I. Postlethwaite, and D. J. Walker, "Nonlinear tracking control for multivariable constrained input linear systems," *Int. J. Control*, vol. 73, pp. 1160–1172, 2000.
- [17] B. M. Chen, T. H. Lee, K. Peng, and V. Venkataramanan, "Composite nonlinear feedback control for linear systems with input saturation: Theory and an application," *IEEE Trans. Automat. Control*, vol. 48, no. 3, pp. 427–439, Mar. 2003.
- [18] W. Lan, C. K. Thum, and B. M. Chen, "A hard-disk-drive servo system design using composite nonlinear-feedback control with optimal nonlinear gain tuning methods," *IEEE Trans. Ind. Electron.*, vol. 57, no. 5, pp. 1735–1745, May 2010.
- [19] F. L. Lewis and V. L. Syrmos, *Optimal Control*, 2nd ed. New York: Wiley-Interscience, 1995.
- [20] Y. X. Su, D. Sun, and B. Y. Duan, "Design of an enhanced nonlinear PID controller," *Mechatronics*, vol. 15, no. 8, pp. 1008–1024, Mar. 2005.
- [21] V. I. Utki, *Sliding Modes in Optimization and Control*. New York: Springer-Verlag, 1992.
- [22] E. F. Camacho and C. Bordons, *Model Predictive Control*. Berlin, Germany: Springer-Verlag, 1998.
- [23] L. Mostefai, M. Denai, and Y. Hori, "Robust tracking controller design with uncertain friction compensation based on a local modeling approach," *IEEE/ASME Trans. Mechatronics*, vol. 15, no. 5, pp. 746–756, Oct. 2010.
- [24] J. Zheng and M. Fu, "Nonlinear feedback control of a dual-stage actuator system for reduced settling time," *IEEE Trans. Control Syst. Technol.*, vol. 16, no. 4, pp. 717–725, Jul. 2008.
- [25] H. Choi, B. Kim, I. Suh, and W. Chung, "Design and robust high-speed motion controller for a plant with actuator saturation," *J. Dyn. Syst., Meas., Control*, vol. 122, pp. 535–541, Sep. 2000.



Zhiyong Chen received the B.S. degree from the University of Science and Technology of China, Hefei, China, and the M.S. and Ph.D. degrees from the Chinese University of Hong Kong, Hong Kong, in 2000, 2002, and 2005, respectively.

He was a Research Associate at the University of Virginia, Charlottesville, during 2005–2006. He is currently a Senior Lecturer at the University of Newcastle, Callaghan, Australia. His research interests include biological and nonlinear systems and control.



Minyue Fu (F'04) received the B.S. degree in electrical engineering from the University of Science and Technology of China, Hefei, China, in 1982, and the M.S. and Ph.D. degrees in electrical engineering from the University of Wisconsin, Madison, in 1983 and 1987, respectively.

From 1987 to 1989, he served as an Assistant Professor in the Department of Electrical and Computer Engineering, Wayne State University, Detroit, MI. He joined the Department of Electrical and Computer Engineering, University of Newcastle, Callaghan,

Australia, in 1989, where he is currently a Chair Professor of electrical engineering. In addition, he was a Visiting Associate Professor at the University of Iowa, from 1995 to 1996, and a Senior Fellow/Visiting Professor at Nanyang Technological University, Singapore, in 2002. His main research interests include control systems, signal processing, and communications.

Dr. Fu has been an Associate Editor the *Automatica*, the *IEEE TRANSACTIONS ON AUTOMATIC CONTROL*, and the *Journal of Optimization and Engineering*.



Aurélio T. Salton received the Bachelor's degree in control systems engineering from the Pontifícia Universidade Católica do Rio Grande do Sul, Porto Alegre, Brazil, in 2007, and the Ph.D. degree from the University of Newcastle, Callaghan, Australia, in 2011.

He is currently a Lecturer at the Pontifícia Universidade Católica do Rio Grande do Sul. His research interests include high-performance controllers and nonlinear systems and control.